

# Multilayer adsorption of lysozyme on a hydrophobic substrate

C. F. Schmidt, R. M. Zimmermann, and H. E. Gaub\*

Physikdepartment der Technischen Universität München, 8046 Garching, FRG

**ABSTRACT** Macromolecular adsorption is known to occur as a complex process, often in a series of steps. Several models are discussed in the literature which describe the microscopic structure of the adsorbate. In the present study we investigated the adsorption of hen egg white lysozyme on alkylated silicon oxide surfaces. A combination of fluorescence excitation in the evanescent field and fluorescence recovery after photobleaching allowed us to measure the amount of adsorbed fluorescent lysozyme and the equilibrium exchange kinetics with molecules in solution. We found that a model with at least three classes of adsorbed mole-

cules is necessary to describe the experimental results. A first layer is formed by the molecules which adsorb within a short time after the beginning of the incubation. These molecules make up ~65% of the final coverage. They are quasi-irreversibly adsorbed and do not measurably exchange with bulk molecules within one day even at temperatures up to 55°C. A second layer, which reaches equilibrium only after several hours of incubation, shows a pronounced exchange with bulk molecules. The on-off kinetics show a distinct temperature dependence from which an activation barrier of  $\Delta E \approx 22$  kcal/mol is derived. A third

layer of molecules that exchange rapidly with the bulk can be seen to comprise ~10% of the total coverage. The exchange rate is on the order of fractions of a second. The binding of the latter two classes of adsorbed molecules is exothermic. From the temperature dependence of the coverage, the binding enthalpy of the slowly exchanging layer was estimated to be  $\Delta H_{\text{ads}} \approx 3.8$  kcal/mol. The second and third class of molecules remain enzymatically active as a muramidase, which was tested by the lysis of the cell walls of *Micrococcus lysodeikticus*. The molecules in the first layer, on the other hand, showed no enzymatic activity.

## INTRODUCTION

The investigation of macromolecular adsorption at liquid/solid interfaces is motivated by a broad range of interests. On the application side, for example, in protein processing, adsorption of proteins may alter the structure and the properties of the molecules (1), but can also change the characteristics of the involved surfaces. In biotechnical or medical applications adsorption characteristics of materials play a crucial role for biocompatibility (2). Especially for implantation materials it is of great importance to understand not only the static structure and composition of the immobilized layer but also the exchange of adsorbed molecules with the surrounding medium (3). Adsorption studies can on the other hand reveal important information about the structure of proteins. Since macromolecules can be exposed to controlled external forces at interfaces, one can, at least in principle, also study internal interactions within the protein (4–6). These interactions may result in complex adsorption processes which are described by a variety of models (1, 3). Hydrophobic interactions generally play an important role in stabilizing the three-dimensional structure of

proteins (7, 8). In the case of T4-lysozyme it has been shown that the thermal stability is mainly determined by the hydrophobic forces between certain regions rich in nonpolar residues (9–11).

In the present study we have investigated the adsorption of hen egg white lysozyme to surfaces that had been rendered hydrophobic by alkylation. Lysozyme was chosen for several reasons. It is an extensively studied, small and stable enzyme (12). The sequence (13, 14) is known, as well as the three-dimensional structure (15) to atomic resolution. Data on thermal stability (16) and reversible denaturation (17) are available. Standard protocols have been worked out to measure its enzymatic activity (18) and allow a quantitative characterization of the functionality of adsorbed and desorbed molecules.

Among the techniques which have been employed to investigate macromolecular adsorption, particularly surface sensitive optics like evanescent wave spectroscopy (19–23) and ellipsometry (24, 25) have led to a better understanding of the adsorption processes. These techniques, however, cannot give any information about the exchange kinetics of adsorbed molecules in chemical equilibrium with bulk molecules. To access the reaction kinetics, we used a combination of total internal reflection

\*To whom correspondence should be addressed.

fluorescence (TIRF) and fluorescence recovery after photobleaching (FRAP) (27, 28). This combination allowed us to determine the number and the exchange of adsorbed molecules by photobleaching their fluorescent labels and subsequently measuring their replacement by unbleached proteins from the bulk solution (21). We have recently further developed this technique by devising a method to internally calibrate the measured intensities and determine absolute coverages (26).

## MATERIALS

### Substrates

Quartz microscope slides (Heraeus Quarzschmelze, Hanau, FRG) were heated to 50°C in detergent (Hellmanex Hellma GmbH and Co., Müllheim, FRG) and rinsed for at least 48 h in deionized water. The surface active contaminants were removed by bubbling clean gas through the water bath. The slides were dried in a vacuum oven at 100°C for 1 h before silanization. Silicon wafers with a natural oxide layer (p type, 1.0.0; Wacker-Chemie GmbH, Burghausen, FRG) were used without further cleaning.

The silanization reaction was carried out following the protocol of Thompson et al. (29). The quartz slides/silicon wafers were dipped in a solution containing hexadecane/tetrachlorocarbon/chloroform/octadecyl trichlorosilane (OTS), (800/120/80/1 by vol). Solvents and OTS were purchased from Sigma Chemical Co. (St. Louis, MO). The reaction was complete after ~1 min as judged by the visible change of the wetting properties of the surface/solvent interface. The substrates were rinsed extensively with chloroform and were allowed to dry for several hours. The silanization was confirmed by measuring the forward contact angle of a water droplet using a horizontal macroscope setup with a CCD camera connected to a digital image processing system (Leutron Vision AG, Glattbrugg, Switzerland). The contact angle was in all cases between 105 and 110°. Quartz beads of 75–150  $\mu\text{m}$  diam (Sigma Chemical Co.) were silanized without further cleaning according to the same protocol.

For each experiment a new slide was used to avoid stray light caused by surface defects.

### Fluorescent protein conjugates

Preparation of 4-chloro-7-nitrobenz-2-oxa-1,3-diazole (NBD) labeled lysozyme and bovine serum albumin (BSA): 100 mg of lysozyme (Sigma Chemical Co.) were dissolved in 10 ml of a pH 7 citrate buffer (0.05 M) (incl. 150 mM NaCl). 570  $\mu\text{l}$  of a 10-mg/ml solution of NBD-chloride (Sigma Chemical Co.) dissolved in DMSO

were added and allowed to react for 1 h at room temperature with constant stirring. 70 mg of BSA (Sigma Chemical Co.) were dissolved in 7 ml of a pH 8.6 borate buffer (0.05 M). 100  $\mu\text{l}$  of a 10-mg/ml solution of NBD-fluoride (Serva Fine Biochemicals Inc., Garden City Park, NY) dissolved in DMSO and were allowed to react in the same way. Unbound label was removed by column chromatography (Sephadex G100) at 4°C in the same buffer as above with the addition of 0.02%  $\text{NaN}_3$ . The labeled protein was stored at 4°C in the dark. The protein concentrations were determined by UV absorption at 280 nm (Lambda 15, Perkin-Elmer Corp., Norwalk, CT), using a specific absorbance of 2.31  $\text{cm}^2/\text{mg}$  in the case of lysozyme and 0.627  $\text{cm}^2/\text{mg}$  in the case of BSA. The specific absorbance was determined with unlabeled protein as NBD shows no significant absorbance at 280 nm. Under the given reaction conditions the labeling ratio is estimated to be ~1:1.

## METHODS

### Total internal reflection fluorescence microscopy combined with photobleaching (TIRFRAP)

The experimental setup for the TIRFRAP measurements will be described in detail in a separate paper (26). A schematic sketch of the principle of the experiment is shown in Fig. 1. It is based on an inverted microscope (Axiomat, Zeiss, Oberkochen, FRG), equipped as a fluorescence microscope. For all experiments we used the 488-nm line of an  $\text{Ar}^+$  ion laser (Innova 70; Coherent Inc., Palo Alto, CA). For the nonbleaching observation of

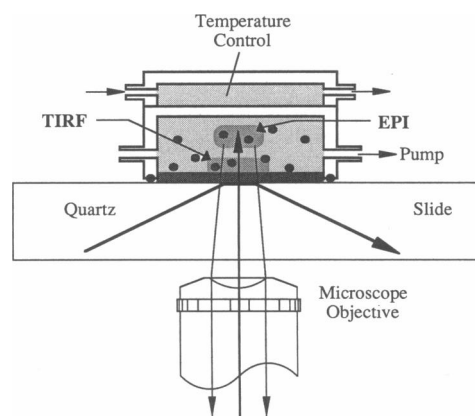


FIGURE 1 Sketch of the principle of the TIRFRAP setup, description in the text.

fluorescence one part of  $\sim 10^{-4}$  of the beam is deviated around the bleaching shutter and can be further attenuated by neutral density filters. A part of the beam is split off and led into the microscope using a conventional EPI-configuration. The main beam is laterally coupled into a quartz microscope slide (preparation see above) via a mirror and a prism which sits on the upper surface of the slide and is optically coupled by immersion oil. The angle of incidence is such that total internal reflection occurs at the glass-air as well as at the glass-water interfaces. The beam is centered and focused by a lens ( $f = 150$  mm) in the field of view of the microscope.

The sample cell is clamped onto the slide and sealed with an O-ring. It has a volume of  $30 \mu\text{l}$ , an accessible area of  $2 \times 15 \text{ mm}^2$  and is designed as a flow chamber to allow the exchange of the bulk solution during the experiment. For that purpose a peristaltic pump is connected to the outlet of the cell.

For temperature control a water bath thermostat (Julabo Labortechnik GmbH, Seelbach, FRG) is connected to a second chamber on top, which is separated from the sample chamber by a wall  $\sim 0.3$  mm thick. The slide mounting is temperature controlled by the thermostat too. For adjustment and control the sample can be observed either via the eye piece or by a sensitive SIT video camera (C2400-08-C; Hamamatsu Corp., Middlesex, NJ). For intensity measurements the fluorescence light from the surface of the quartz slide is focused onto a pinhole in front of a photomultiplier (C 31034 RCA). The observed area is thus limited to a circular spot  $70 \mu\text{m}$  in diameter. The photomultiplier is operated in photon counting mode, pulses are counted by custom-made electronics interfaced to a microcomputer (Apple II).

We used the setup in two modes of operation: For the simultaneous observation of bulk and surface fluorescence the bleach shutter is closed and the shutters for TIRF- and EPI-illumination are alternately opened and closed. The duration of sample intervals and breaks is variable. A typical shutter-open time was 200 ms with a break of some seconds. Photobleaching experiments were carried out under TIRF-illumination (TIRFRAP). Bleaching times can be chosen between  $\sim 20$  ms and a couple of seconds. Overall recording times can vary from  $\sim 1$  s to  $\sim 1$  h. In both modes of operation the recorded intensities, corrected for background light, are stored for further evaluation.

### Evanescent field geometry

The evanescent field of the reflected beam decays exponentially on the solution side with a decay constant on the order of  $1,500 \text{ \AA}$  in the geometry we used. A sketch of the geometry is shown in Fig. 2. The penetration depth can be

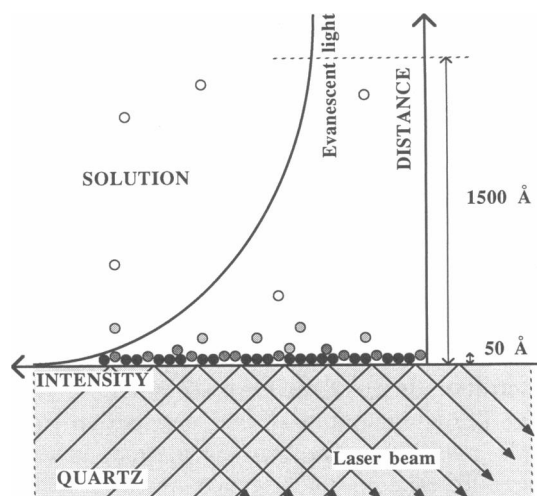


FIGURE 2 Sketch of the geometry of the evanescent field with a surface coverage by protein as determined for lysozyme, approximately to scale.

calculated for each experiment from the angle of incidence at the reflecting surface (22). Consequently, provided the bulk concentration of labeled molecules is high enough, there will be a substantial contribution from free bulk molecules to the TIRF signal. Under certain conditions this bulk contribution can be separated from the contribution of adsorbed molecules provided these two populations of molecules have different mobilities. This can either be done in a photobleaching experiment or by flushing the chamber with buffer or a solution of unlabeled molecules. In a FRAP experiment bulk molecules show up as an apparently unbleachable base in the fluorescence signal. This is because diffusion over the distance of  $1,500 \text{ \AA}$  is usually too fast to be resolved by the apparatus. The complete bleaching of the immobile molecules can be achieved by consecutive short bleach pulses. This method is easy to apply, if there is no fast (in the order of seconds) exchange process involving adsorbed molecules. A serious limitation arises if an exchange process lies in the order of magnitude of the bleach pulse duration. Because free molecules that are bleached near the surface have to be exchanged by essentially one-dimensional diffusion, a depletion layer of fluorescent molecules is created at the surface. In a first approximation it takes about the same time to fill that concentration hole as it took to create it, i.e., the duration of the bleach pulse (30). Within this time the exchange of adsorbed molecules must be negligible to obtain the correct value for the bulk contribution.

Flushing the chamber avoids the depletion effect, but results in a chemical nonequilibrium situation and can

only be used to measure the bulk contribution if the other exchange processes are slower than ~20 s.

With the known field geometry and bulk concentration the fluorescence signal from surface bound molecules can be readily converted into absolute coverage data by comparison with the bulk contribution (described in detail in reference 26):

$$c_a = \frac{c_0 d}{2} \left( \frac{I_F}{I_F^B} - 1 \right), \quad (1)$$

where  $c_0$  is the bulk protein concentration in mg/ml,  $d$  is the penetration depth of the evanescent field in cm,  $I_F$  is the total TIRF signal and  $I_F^B$  the contribution from the free bulk molecules. For this calculation, however, a possible difference in fluorescence quantum efficiency between free and adsorbed molecules has to be taken into account.

## Ellipsometry

The apparatus for the ellipsometrical measurements is described elsewhere in detail (31). It is a custom-made device operating in zero-ellipsometry mode at a fixed incidence angle of 70° and a wavelength of 632 nm (He-Ne laser; Uniphase, Nanteca). A chamber with windows perpendicular to the beams allows us to measure adsorption from a bulk fluid. The measured parameters are the inverse tangent of the reflexivity ratio  $\Psi$  and the phase shift  $\Delta$  of the  $s$ - and  $p$ -polarized components of the reflected wave. These values were compared with simulated data based on a system of multiple layers of different complex refractive indices  $\hat{n}$ . Simulation was carried out on a microcomputer (IBM AT) by solving the complex Fresnel equations.

The silicon wafers used as substrate ( $\hat{n} = \{3.80, -0.09\}$ ) had a natural oxide layer ( $\hat{n} = \{1.47, 0\}$ ) of 14 Å average thickness measured in air. After silanization the hydrocarbon layer ( $\hat{n} = \{1.54, 0\}$ ) showed a thickness of 14 Å, again measured in air.

The adsorbed protein layer was modeled as a homogeneous layer with a complex refractive index of  $\hat{n} = \{1.55, 0\}$ . The refractive index of the buffer was  $\hat{n} = \{1.34, 0\}$ .

## Thermal denaturation of lysozyme

The thermal denaturation of lysozyme was observed by 90° light scattering in a fluorescence spectrometer at 400 nm (Spectrofluorometer RRS 1000, Schoeffel Instr. Corp., Westwood, NJ). A 10 × 10 mm fluorescence cell (Hellma, Müllheim, FRG) was filled with 3 ml of a protein solution (4.5 mg/ml) in pH 7 citrate buffer and was placed in the sample holder of the spectrometer,

which was thermostatically controlled by a water bath (Lauda, FRG). The temperature was increased at a constant rate of 1°C/min. Before denaturation occurred, the temperature was decreased again to check for reversibility and was then increased until denaturation could be seen as a steep increase in the scattered intensity caused by protein aggregation.

## Enzymatic activity of lysozyme

Lysozyme is a muramidase and lyses the outer coat of certain bacteria, whereupon the cell membrane is disrupted by osmotic pressure. This activity can be quantified by turbidity measurements of a bacteria suspension. The relative decrease of the turbidity of the solution is a linear function of the enzymatic activity. The quantitative analysis of the enzymatic activity of lysozyme was performed according to the protocol described by B. Weisner (18). We used a suspension of *Micrococcus lysodeikticus* (Sigma Chemical Co.) as substrate. Instead of turbidity, as in the standard protocol, we measured the scattered light at an angle of 90° in a fluorescence spectrometer (Fluorolog2, Spex Industries, Inc., Edison, NJ) using a 10 × 10 mm quartz fluorescence cell (Hellma). The monochromators for excitation and detection were set to 450 nm. The cell was placed in a brass block which was thermostatically controlled by a water bath (Julabo Labortechnik, Seelbach, FRG). After mixing the sample solution, the scattered intensity was continuously recorded either at a fixed temperature or during the heating of the sample with a fixed heating rate. The enzymatic activity of adsorbed lysozyme was determined by using microscopic quartz beads of 75–150 μm diam (Sigma Chemical Co.) as follows. The quartz beads were alkylated with OTS as described above. The cell was filled with 2.4 ml of a solution of fluorescent labeled lysozyme and the fluorescence intensity was measured with excitation at 468 nm and detection at 520 nm. 1 g of beads was added and incubated for 1 h at room temperature with frequent stirring by inverting the cell. After the beads had sedimented to the bottom of the cell, the fluorescence intensity was measured again. From the difference in fluorescence the adsorbed quantity of protein was determined. After removing the excess protein by extensive washing with buffer, 3 ml of bacteria suspension were added. The scattering intensity at constant temperature was recorded as above with the glass beads sedimented on the bottom of the cell. The sample was intermittently stirred by inverting the cell. The recording was started again after a 60-s break to allow the beads to settle. As a control the effect of uncoated and of bovine serum albumin coated glass beads on the bacterial solution was measured in an analogous way. No significant

decrease in the scattered intensity could be detected (see Fig. 9).

## RESULTS AND DISCUSSION

### Fluorescent labeled lysozyme

A considerable amount of literature has been published on protein adsorption measured by evanescent field fluorescence spectroscopy. In most cases intrinsic tryptophan fluorescence has been used which has the advantage that the native molecule can be studied. For photobleaching techniques, however, where the light absorbing part of the molecule is irreversibly destroyed, a method using externally attached labels offers several advantages. (a) The molecules of interest can be selectively labeled and thus measured in the presence of other types of proteins. This is of interest for example, in competitive adsorption experiments. (b) The protein itself does not absorb at the wavelength at which the common fluorescent labels are excited. This keeps radiation damage to a minimum. (c) The group which is irreversibly destroyed by bleaching can be chosen in such a way that the functions of the native protein are not drastically disturbed. We used an NBD-label which is known to bind to proteins predominantly via cysteines and free amino groups (32, 33).

To quantify the changes in the molecular properties of lysozyme induced by the fluorescent labeling we have compared the thermal properties of the labeled and the native protein. The result is shown in Fig. 3. Thermal denaturation was measured by static light scattering as described in the methods section. Both labeled and native lysozyme were stable up to  $>70^{\circ}\text{C}$  and showed a slight increase in scattering intensity which was reversible upon cooling. Above  $\approx 73^{\circ}\text{C}$  irreversible aggregation occurred. In the whole temperature scan we found no significant difference between labeled and native lysozyme.

In a separate experiment we measured the enzymatic activity of the protein. We recorded the  $90^{\circ}$  scattering intensity of a bacterial suspension incubated with the enzyme as described in the methods section above. To compare labeled and unlabeled lysozyme, we measured the temperature dependence of the enzymatic activity of both protein species at the same concentration (5.7 nM). In a single scan the temperature was varied from 35 to  $70^{\circ}\text{C}$  at a constant rate of  $3^{\circ}\text{C}/\text{min}$ . The total scan duration was chosen to be short enough to ensure that the intensity decrease would be approximately linear in time if it were at a constant temperature. This was tested in separate experiments (data not shown). Consequently the slopes of the curves ( $\square$ ) and ( $\blacksquare$ ) in Fig. 3 are directly proportional to the enzymatic activity at the respective temperatures. Again the differences between labeled and

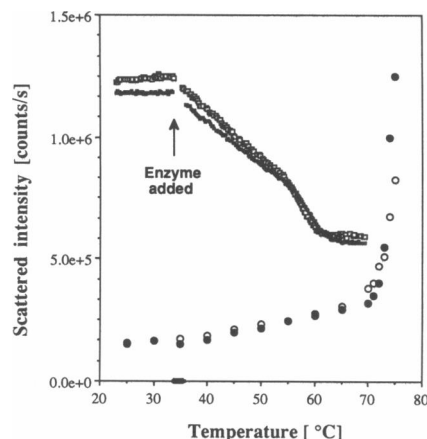


FIGURE 3 Thermal denaturation of native and NBD-labeled lysozyme. The  $90^{\circ}$  light scattering signal (400 nm) of a solution of native (O) and NBD-labeled ( $\bullet$ ) was measured as a function of temperature in a fluorescence spectrometer. The protein concentration was 4.5 mg/ml in pH 7 citrate buffer. After heating the sample to  $70^{\circ}\text{C}$  (at a rate of  $1^{\circ}\text{C}/\text{min}$ ) it was cooled again to check for irreversibility before finally increasing the temperature to  $75^{\circ}\text{C}$ .

The temperature dependence of the enzymatic activity of native ( $\square$ ) and NBD-labeled ( $\blacksquare$ ) lysozyme was measured by the change in  $90^{\circ}$  light scattering of a suspension of *Micrococcus lysodeikticus* in a fluorescence spectrometer at 450 nm wavelength. The enzyme concentration was 5.7 nM, the temperature was increased at a constant rate of  $3^{\circ}\text{C}/\text{min}$ .

native molecules are marginal. It is interesting to note that both plots show an increase in slope at  $\sim 55^{\circ}\text{C}$  which indicates an increase in the efficiency of the reaction above that temperature. At present we do not know whether this is due to the substrate or to the enzyme. Above  $T \approx 63^{\circ}\text{C}$  no enzymatic activity is detectable. The two described experiments show that our labeling procedure did not alter the thermal properties of lysozyme. These experiments also define a temperature range of up to  $T \approx 55^{\circ}\text{C}$  within which we do not expect any structural changes in the protein. In the range from  $T = 55^{\circ}\text{C}$  to  $63^{\circ}\text{C}$  we know that the protein is functional, but it might have different properties which might also be reflected in the adsorption behavior.

### Adsorption to hydrophobic substrates

As described in the methods section the absolute quantity of adsorbed molecules can be measured by TIRFRAP. To quantify a possible difference in the fluorescence quantum yield between free and adsorbed molecules, we also measured the adsorption of lysozyme to OTS-alkylated silicon oxide by ellipsometry. Fig. 4 shows the time courses of adsorption determined both by ellipsometry and by TIRF. Both curves exhibit a comparable time

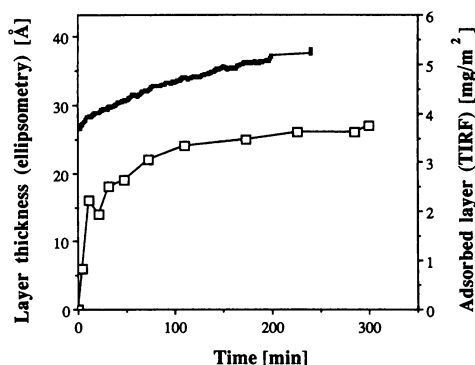


FIGURE 4 Adsorption kinetics of NBD-labeled hen egg white lysozyme onto alkylated silicon oxide. The lower curve ( $\square$ — $\square$ ) was measured with ellipsometry at 20°C and a bulk concentration of native lysozyme of 5 mg/ml in pH 7 citrate buffer. The layer thickness in Å is given on the left-hand scale. The upper curve ( $\blacksquare$ — $\blacksquare$ ) was measured by TIRF with NBD-lysozyme at a bulk concentration of 0.42 mg/ml in pH 7 citrate buffer at a temperature of 40°C. The mass coverages marked on the right-hand scale were calculated from the fluorescence intensities as described in the text. The two axes are scaled in a way that the layer thickness corresponds to the respective mass coverage for a specific density of the adsorbate of 1.39 g/cm<sup>3</sup>.

dependence of the adsorption. A fast initial increase within minutes, corresponding to about half of the final coverage, is followed by a slow increase over several hours. The difference in the time dependence of the curves is probably largely due to the different measuring temperatures (40°C for TIRF, 20°C for ellipsometry). Ellipsometry measures an end value in the thickness of  $27 \pm 3$  Å. TIRFRAP gives a final coverage of  $5.3 \pm 0.5$  mg/m<sup>2</sup>. Layer thickness can be directly converted in mass coverage and vice versa by assuming a specific density of the protein. The measured values are consistent with each other, assuming a protein density of  $\approx 1.9$  g/cm<sup>3</sup>. Although this value lies within the range of values given in the literature for adsorbed proteins, it seems unreasonably high to us. Assuming a value of  $\approx 1.4$  g/cm<sup>3</sup> for the specific density seems more realistic, compared with specific densities measured for proteins in solution, since it corresponds already to an almost dense packing. Using this specific density, however, gives rise to a discrepancy between measured mass coverage and layer thickness of  $\sim 30\%$ . The ordinates in Fig. 4 are scaled in a way that the layer thickness in Å on the left-hand axis corresponds to the respective surface density in mg/m<sup>2</sup> for a specific density of the adsorbate of 1.39 g/cm<sup>3</sup>. This is a measured value for lysozyme in solution (34). One reason for this deviation between the results for the final coverage might be a change in the quantum yield of the fluorescent label upon adsorption, but the good agreement of our value with literature values obtained from measured trypto-

phan fluorescence (see below) makes this seem unlikely. Another more probable reason for the discrepancy lies in the interpretation of the measured values of  $\Delta$  and  $\Psi$  in ellipsometry. The optical model for the Fresnel calculation, which is used to correlate the measured angles with thickness and refractive index of the adsorbate layer, assumes step functions in the complex refractive index between the layers. This is known to be at best a rough approximation leading to refractive indices for the adsorbate of up to 2.0, which is hardly acceptable. Unfortunately no better models are available at present. Thus all the determined absolute values are subject to this systematic uncertainty and we have to assume that the range of error in determining the absolute coverage is about as large as the difference between the results of the two techniques.

We are not aware of literature data for lysozyme adsorbed to alkylated surfaces. From adsorption studies onto dimethyl silane an average coverage of  $\sim 5$  mg/m<sup>2</sup> has been reported (35). On various metal surfaces coverages between 3.9 mg/m<sup>2</sup> and 5.1 mg/m<sup>2</sup> were found determined by capacitance measurements (25). Thus the coverage measured in our experiments seems to be within the range expected for lysozyme adsorption. X-Ray data from lysozyme give an ellipsoidal geometry of  $\sim 45 \times 30 \times 30$  Å<sup>3</sup> (15). It is interesting to note that the measured coverage corresponds roughly to a monomolecular layer although below it will be shown that, judged from the molecular mobility, the adsorbed layer is composed of different populations of molecules.

## Exchange kinetics

After the samples had been allowed to equilibrate for  $\sim 4$  h at 40°C, the kinetics of the desorption-adsorption equilibrium were investigated in a TIRFRAP experiment. It is assumed that the exchange kinetics are not influenced by the photobleaching process (which will be discussed later in detail). Under equilibrium conditions the off rate equals the on rate and is given directly by the recovery time of the fluorescence provided the contribution of rebound bleached molecules is negligible. The time course of such an experiment at a temperature of 55°C is plotted in Fig. 5, curve I. With a brief laser pulse (500 ms) of high intensity ( $10^3$  W/cm<sup>2</sup>) the fluorescent labels of the proteins within range of the evanescent field were bleached. The subsequent recovery of the fluorescence, detected by TIRF, shows three clearly distinguishable time domains. In a first fast process  $\sim 10\%$  of the bleached intensity recovers within tens of seconds. A second process brings back  $\sim$  another 25% with a characteristic time of  $\sim 1,500$  s. About 65% of the bleached fluorescence does not recover within the duration of the experiment. There is also a base of apparently unbleachable fluorescence

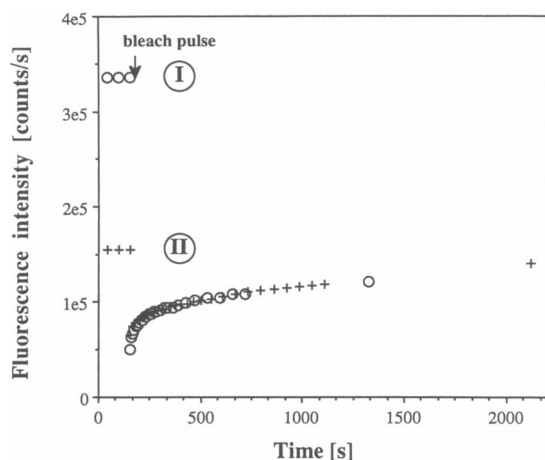


FIGURE 5 Fluorescence recovery traces from adsorbed lysozyme after a 300-ms bleach pulse in TIRF. Curve I was measured at 55°C with a sample that had been incubated with NBD-labeled lysozyme (0.42 mg/ml in pH7 citrate buffer) for 4 h at 40°C as shown in Fig. 4. Curve II was also measured at 55°C, but the sample had been incubated with native lysozyme (10 mg/ml in pH 7 citrate buffer) overnight before the bulk was exchanged for a solution of NBD-labeled lysozyme (0.42 mg/ml in pH7 citrate buffer).

caused by the fast exchange of free bulk molecules, as the even evanescent field reaches  $\sim 1,500 \text{ \AA}$  into the bulk (for details cf. reference 26). A possible artifact would be that irreversible photocross-linking due to the high laser intensities immobilizes the majority of the adsorbed proteins. To test for such an effect, we first incubated the surface with native lysozyme for 12 h at room temperature and then added fluorescent lysozyme. The TIRFRAP experiment, plotted as curve II in Fig. 5, was carried out after another 6 h of incubation. Within the experimental error the two curves are congruent except that the immobile part is missing in the case of the preincubated surface. Because a recovery of 100% was measured in the case of the preincubated surface, photocross-linking can be ruled out as the reason for the large immobile fraction. On the other hand, because curve I does not deviate from curve II even at long times, the experiment shows that the molecules which adsorb to the surface in the beginning of the incubation are quasi irreversibly attached, and only the molecules which bind in the subsequent slow process are in equilibrium with the bulk phase. Whether the latter population of molecules intercalates in the base layer and binds directly to the surface or adheres to already adsorbed protein cannot be decided from the data.

To determine the thermodynamic parameters of this complex adsorption process, we investigated the temperature dependence of the exchange kinetics. A series of experiments like the one in Fig. 5 was carried out over a range of temperatures. A logarithmic plot of the corre-

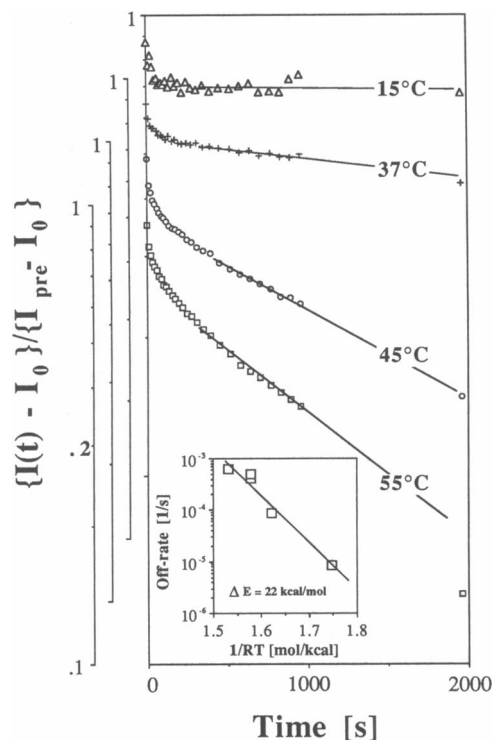


FIGURE 6 Logarithmic plot of TIRFRAP recovery curves measured at various temperatures with NBD-labeled lysozyme adsorbed on top of a layer of native lysozyme on alkylated quartz. The bulk protein concentration was 0.9 mg/ml in pH 7 citrate buffer. The normalized curves,  $\{I(t) - I_0\} / \{I_{pre} - I_0\}$ , are vertically shifted like the ordinate scales.  $I_{pre}$  is the measured prebleach intensity and  $I_0$  is the intensity directly after bleaching. The drawn lines are calculated from a linear regression through the long time parts of the curves. (Insert) Arrhenius plot of the exchange rates of NBD-labeled lysozyme adsorbed on top of a layer of native lysozyme on alkylated quartz. The exchange rates were determined from linear regressions through the long time parts of the logarithmically plotted, normalized TIRFRAP recovery curves shown above. The activation energy,  $\Delta E$ , was determined by linear regression.

sponding TIRFRAP curves is given in Fig. 6. The fast and the slow exchange processes are again clearly separable. Because the recovery of the bulk depletion layer cannot be separated from a fast exchange process of adsorbed molecules (see Methods), a possible temperature dependence of the fast process cannot be resolved. The kinetics of the slow process, however, clearly show a pronounced temperature effect. With increasing temperature the exchange rate increases dramatically, showing the process to be thermally activated. Assuming as a first approximation a two-state reaction with an activation barrier of height  $\Delta E$ , we can determine  $\Delta E$  from an Arrhenius plot of the exchange rates measured in the FRAP experiments. This is shown in the insert of Fig. 6. The slopes of the long time parts of the logarithmically plotted recovery curves were taken as rate constants.

From the slope of a linear regression through the data points the activation energy  $\Delta E$  was calculated to be  $\Delta E = 22$  kcal/mol (see insert of Fig. 6). This activation barrier indicates that some (reversible) conformational changes occur in the protein. From calorimetric measurements the change in Gibbs free energy accompanying the thermally induced unfolding of lysozyme has been determined to be  $\approx 10$  kcal/mol (36). This shows that the activation barrier measured in our experiments is in the order of magnitude of the energy necessary for conformational changes.

The equilibrium constant of the slow exchange process can be derived from the amplitude of this process. From the temperature dependence of this equilibrium constant the binding enthalpy can be calculated. In contrast to the rate constants which are independent of absolute intensities and therefore of the quantum yield of the dye, the recovery amplitudes have to be corrected for temperature dependent fluorescence quenching. For this purpose the temperature dependence of the fluorescence was measured for several systems: adsorbed NBD-lysozyme and adsorbed NBD-BSA were measured in TIRF excitation. NBD-BSA was heated in the presence of protein in the bulk and cooled with buffer in the bulk. Measured intensities during cooling are plotted in Fig. 7. NBD-lysozyme was incubated at  $40^\circ\text{C}$ , heated to  $55^\circ\text{C}$ , and cooled without protein in the bulk. For the same samples, before flushing the bulk, the bulk intensities were measured using EPI illumination during heating. All four curves are plotted logarithmically versus temperature in Fig. 7. All curves show essentially the same slope which means that the fluorescence is thermally quenched with about the same temperature factor in all four cases. For an unknown reason the slope of both the TIRF curves is slightly smaller than that of the bulk curves. The slope of the lysozyme TIRF curve corresponds to an exponential decay rate of  $8.5 \times 10^{-3} \text{ }^\circ\text{C}^{-1}$ . This value was used to correct measured fluorescence amplitudes for thermal quenching.

Due to the fast exchange process and a limited bleaching depth the determination of the amount of the slowly mobile molecules from FRAP curves as shown in Fig. 5 were affected by a large experimental error. Therefore, by a series of flushing experiments, we also measured the temperature dependence of the coverage made by these molecules. For these measurements a sample was used that had been incubated overnight with native lysozyme, as described above. The surface was then incubated with labeled lysozyme for 4 h at  $40^\circ\text{C}$ . In several steps the temperature was decreased to  $3.6^\circ\text{C}$ , pausing at each temperature for 1–2 h until equilibrium was reached. Finally the sample was heated again to  $40^\circ\text{C}$  to check reversibility. After 1 and 2 d the sample was measured

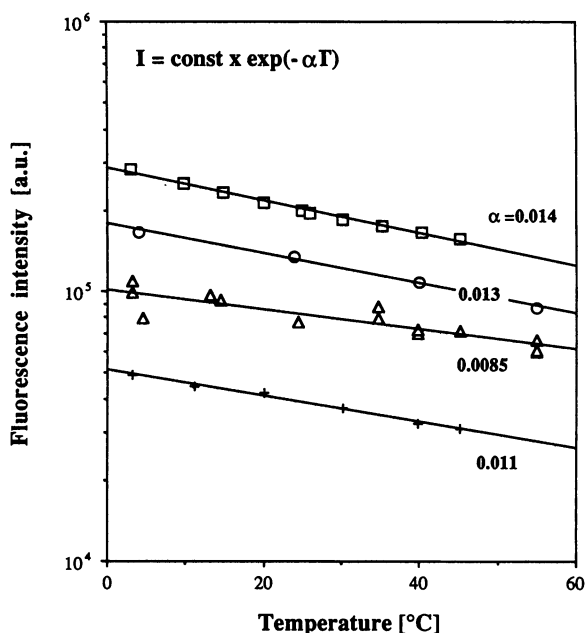


FIGURE 7 Temperature dependence of fluorescence quenching for protein solutions (measured in EPI-illumination) and for adsorbed protein (measured in TIRF-illumination). The samples were heated and cooled in several steps and measured after equilibration at every temperature. ( $\square$ ) NBD-labeled BSA (1 mg/ml in pH 7 PBS buffer), EPI-signal (bulk) during heating. (+) Same sample, TIRF-signal (surface) measured after flushing the bulk with buffer at  $45^\circ\text{C}$ , during cooling. ( $\circ$ ) NBD-labeled lysozyme (0.42 mg/ml in pH 7 citrate buffer), EPI-signal (bulk), during heating. ( $\Delta$ ) same sample, TIRF-signal (surface) measured after flushing the bulk with buffer at  $55^\circ\text{C}$ , during cooling. The drawn lines are linear regressions through the logarithmically plotted data points, quenching rates are given for each sample.

again at  $20^\circ\text{C}$ ,  $40^\circ\text{C}$ , and  $3.8^\circ\text{C}$  to check for long time stability.

At each temperature the fluorescence intensity was measured at several not yet illuminated spots on the sample, before and after exchanging the bulk solution for buffer. The measured intensities proved to be reproducible at the respective temperatures with  $\approx 20\%$  variance (a) at different spots on the surface, (b) after cooling and heating again, and (c) over the 2 d of the experiment.

In Fig. 8 a the average intensities (scale on the left-hand side) from the slowly exchanging molecules, corrected for thermal quenching, are plotted against temperature (curve I). The absolute coverage on the right-hand axis was estimated by internal calibration against bulk molecules as described below in detail. Also plotted in Fig. 8 a are the average temperature-corrected intensities from quickly exchanging molecules, which are given by the height of the step in intensity seen upon flushing the chamber with buffer at the respective temperatures



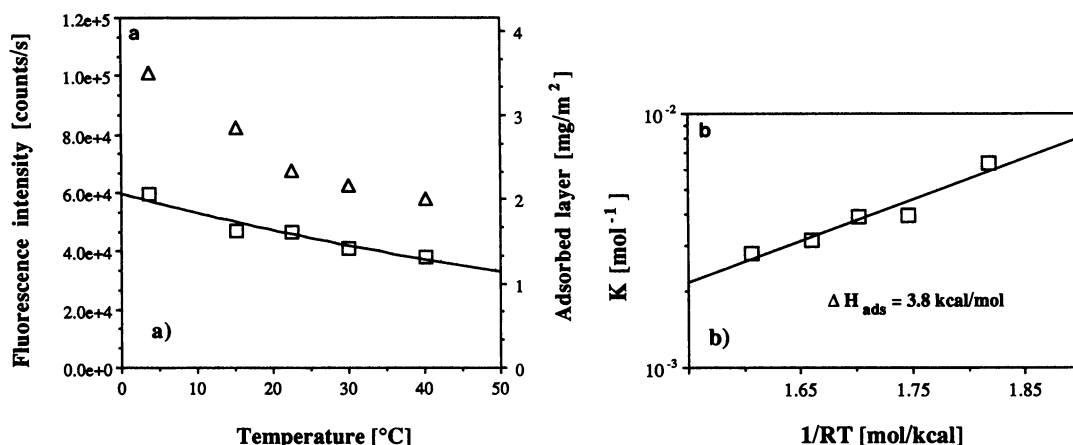


FIGURE 8 (a) Temperature dependence of surface coverages, curve I (□): slowly mobile layer, curve II (Δ): highly mobile layer, including the contribution from free bulk molecules. Fluorescence intensities were measured in flushing experiments with a sample that had been incubated with native lysozyme (10 mg/ml in pH 7 citrate buffer) overnight before the bulk was exchanged for a solution of NBD-labeled lysozyme (2.8 mg/ml in pH 7 citrate buffer). The sample was equilibrated for 1–2 h at the various temperatures. The temperature was increased and decreased to check for reversibility and the sample was observed for 2 d to check for very slow processes. The plotted data points are average values at the respective temperatures, corrected for thermal quenching by using the quenching rate determined in Fig. 7 for adsorbed lysozyme. As a measure for the slowly and highly mobile fraction the fluorescence intensity directly after flushing the bulk with buffer and the intensity step height during the flushing were taken respectively.

(b) Van't Hoff plot of the equilibrium constants of the adsorption reaction of the slowly exchanging class of molecules, calculated from the data shown in Fig. 8 a as described in the text. The binding enthalpy  $\Delta H_{\text{ads}}$  was determined from a linear regression (drawn line).

(curve II). The amount of these quickly exchanging molecules is also temperature dependent. This indicates that in addition to free bulk molecules, molecules that are loosely attached to the surface in an exothermic reaction contribute to this effect.

As a check for the reversibility of the exchange, labeled molecules in the bulk were replaced by native molecules. It should be noted that even at higher temperatures the exchange of adsorbed labeled proteins against unlabeled proteins from the bulk occurs more slowly than the exchange of labeled proteins as seen in the TIRFRAP experiments. Although labeled and native molecules were virtually indistinguishable with respect to enzymatic activity and thermal stability, there is clearly a difference between the molecules with respect to their affinity for the surface.

The binding enthalpy of the slowly exchanging class of molecules was estimated by a van't Hoff plot of the equilibrium constants,  $K(T)$ , calculated from the intensities given in Fig. 8 a, to be  $\Delta H_{\text{ads}} \approx 3.8$  kcal/mol (cf. Fig. 8 b).

The application of the van't Hoff equation to determine the binding enthalpy,  $\Delta H_{\text{ads}}$ :

$$\frac{d}{dT} \ln K = \frac{\Delta H_{\text{ads}}}{RT^2}, \quad (2)$$

requires reversibility and isosteric conditions. The first requirement is fulfilled, whereas the latter cannot be controlled. Therefore the value for  $\Delta H_{\text{ads}}$  is a rough estimate. Nevertheless Le Chatelier's principle is still applicable. Therefore the exothermic character of both reactions (the quickly and the slowly exchanging molecules) is clearly established by the data.

Although the above mentioned limitations may make the result seem ambiguous, the formalism used to determine the equilibrium constants is given in detail to illustrate the general approach. In order to calculate the equilibrium constants plotted in Fig. 8 b, a simple model was assumed to describe the adsorption reaction, namely that free proteins ( $P$ ) and free binding sites on the surface ( $S$ ) are in equilibrium with 1:1 complexes of proteins and binding sites ( $PS$ ).



$$K = \frac{[PS]}{[P][S]}, \quad (4)$$

where the brackets denote surface and volume concentration, respectively.

The concentration of binding sites was assumed to be

limited to the number resulting from a monomolecular coverage of the surface:

$$[S]_{\max} = [PS]_{\max} = \text{dense monomol packing} \quad (5)$$

$$\rightarrow [S] = [PS]_{\max} - [PS]. \quad (6)$$

To determine the concentrations, we had to calculate absolute coverages from the measured intensities. Because of the presence of the highly mobile layer, which conceals the contribution of free bulk molecules at low bulk concentrations, the internal calibration was performed in flushing experiments with high bulk concentrations by varying this concentration. This was done with a sample containing only labeled lysozyme. That means that the major part of the signal stemmed from irreversibly adsorbed molecules. We therefore neglected a possible change of the amount of slowly mobile molecules with the bulk concentration. Having calculated the coverage from the two lower layers of molecules to be  $5.3 \pm 1 \text{ mg/m}^2$  at  $20^\circ\text{C}$ , we estimated the separate contributions from FRAP curves like the one shown in Fig. 5 to be  $3.7 \text{ mg/m}^2$  (70%) for the immobile and  $1.6 \text{ mg/m}^2$  (30%) for the slowly exchanging fraction at  $20^\circ\text{C}$ . Assuming  $3.7 \text{ mg/m}^2$  also to be a maximum coverage for the slowly exchanging fraction and using the value of  $1.6 \text{ mg/m}^2$  to calibrate curve I in Fig. 8 a, the data points in Fig. 8 b were calculated according to Eqs. 4 and 6.

The binding enthalpy for the fast fraction could not be estimated in a similar way, as the error introduced by separating the contribution of free bulk molecules from that of loosely attached molecules in curve II, Fig. 8 a, proved to be too large. From FRAP curves like the one shown in Fig. 5 we estimated 10% to be an upper limit of the relative amount of the fast fraction. As there is no activation barrier seen in this process, it seems that no conformational changes are involved. It is known that lysozyme has a weak tendency to dimerize at a pH between 5 and 9 (17). This way of binding between protein and protein may be responsible for the observed loosely bound layer.

## Enzymatic activity

From the preceding results we have seen that a major part of the lysozyme adsorbed to the hydrophobic surface is irreversibly bound. We do not have any information about accompanying structural changes in the protein. It is very probable, however, that the interaction with the hydrophobic surface leads to a partial unfolding of the protein. The hydrophobic core that stabilizes the three-dimensional structure of the protein in aqueous solutions would thus be exposed to the surface. One of the reasons why we chose an enzyme as a model molecule is that its structure is directly related to its function, which is relatively easy

to probe. A test of the enzymatic activity of the adsorbed molecules should thus provide information about structural changes.

The plane geometry used up to now has advantages for optical purposes, but results in a small total surface. The total amount of adsorbed enzyme is too small to lyse bacteria at a measurable rate. We therefore alkylated microscopic quartz beads in the same way as the microscope slide surface in the experiments above. Glass beads were loaded with an excess of lysozyme to ensure maximal surface coverage and then washed. At room temperature, the rate for the slow exchange of the top layer of molecules is on the order of hours, so that coverage persists until incubation with a *Micrococcus* solution (see also Methods). The light scattering signal from the bacterial suspension at a constant temperature of  $25^\circ\text{C}$  is shown in Fig. 9 (curve III). As a control the effect of the pure uncovered glass beads was also measured (curve I). In a second experiment the same amount of glass beads was incubated with only 60% of the lysozyme necessary for maximal coverage. The light scattering signal of a bacterial suspension incubated with these beads is also plotted in Fig. 9 (curve II). The first sample showed an enzymatic activity which approximately equaled that of a test solution containing 1.7% of the amount that was

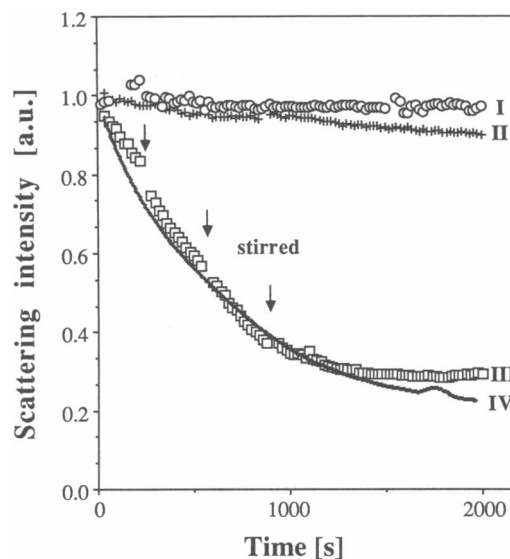


FIGURE 9 Enzymatic activity of NBD-lysozyme adsorbed to alkylated quartz beads, measured by the decrease in  $90^\circ$  light scattering (450 nm) of a bacteria suspension at  $25^\circ\text{C}$ . Curve I (O) shows the effect of the pure, uncoated glass beads, curve II (+) shows the activity of 60% covered beads, and curve III ( $\square$ ) that of 100% covered beads. For comparison, curve IV ( $\blacksquare$ ) shows the enzymatic activity of a 19.8 nM solution of lysozyme (corresponding to  $\approx 1.7\%$  of the amount of the lysozyme adsorbed to the quartz beads in curve III) under equivalent experimental conditions.

adsorbed on the glass beads (*curve IV*). In the second experiment, with 60% coverage of the beads no significant enzymatic activity could be seen. This means that the first layer shows virtually no enzymatic activity, whereas the molecules adsorbed on top can presumably desorb slowly into the solution again in a functional form. The fact that the enzymatic reaction continues when the beads have settled on the bottom of the cell indicates that enzymes are present in the solution again. Moreover, the slope of the curve becomes slightly steeper after each break during which the solution had been stirred. This also shows that enzymes desorb slowly from the surface.

## CONCLUDING REMARKS

The above experimental findings are summarized in Fig. 10. The first layer of adsorbed lysozyme is quasi irreversibly bound and shows no enzymatic activity. As the average mass coverage is only ~60% of a monomolecular layer, we assume that due to the strong interaction with the hydrophobic interface the protein unfolds and the normally buried hydrophobic domains of the protein contact the substrate. Subsequently adsorbed molecules are enzymatically active and exchange in a thermodynamic equilibrium with molecules in solution. Two different kinetics characterize this exchange process. For the major part of these molecules the exchange is hindered by an activation barrier, and the characteristic exchange times are on the order of 1,000 s. A minority of these molecules exchanges within seconds.

Both reactions are exothermic as judged from the temperature dependence of the coverages. The binding enthalpy of the slow process was estimated to be 3.8 kcal/mol. The activation barrier was determined to be 22 kcal/mol. In our model this slow exchange is performed by molecules which "see" less of the surface than those of the first layer. The high activation barrier, however,

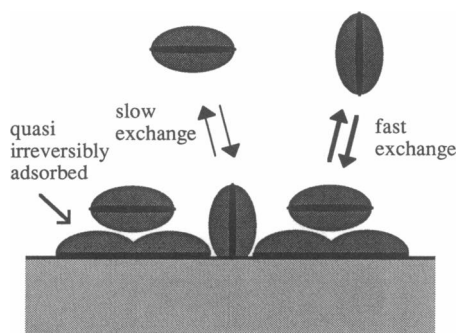


FIGURE 10 Proposed model of three layered adsorbate structure of lysozyme on a hydrophobic substrate.

indicates that some (reversible) conformational changes still occur in the protein. The fast exchanging molecules just loosely adhere to the surface in our model, and the lack of an activation barrier makes it likely that in this case no conformational changes are involved. The known tendency of lysozyme to form dimers could be due to the same binding mechanism.

One of the major purposes of the present study was to demonstrate that the combination of fluorescence photobleaching and excitation in the evanescent field provides a unique technique which allows us to investigate macromolecular adsorption in a very detailed manner. The main advantages turned out to be the ability to measure both the magnitude and the kinetics of exchange processes in thermodynamic equilibrium. We think that this technique will be applicable not only for the investigation of macromolecular adsorption phenomena, but also to a broad range of related problems. Examples are specific receptor-ligand interactions with one of the reactants immobilized at the surface and specific macromolecular reactions on biological cell surfaces, which can be mimicked by supported lipid membranes.

This work was supported by the Deutsche Forschungsgemeinschaft. We would like to thank Erich Sackmann, Erwin Killmann, Dean Madden, and Dan Leahy for helpful discussions.

Received for publication 10 July, 1989 and in final form 9 November, 1989.

## REFERENCES

1. Andrade, J. D., and V. Hlady. 1986. Protein adsorption and materials biocompatibility. *Adv. Polym. Sci.* 79:1-63.
2. Andrade, J. D., S. Nagaoka, S. Cooper, T. Okano, and S. W. Kim. 1987. Surfaces and blood compatibility. *Trans. Am. Soc. Artif. Intern. Organs.* 33:75.
3. Vroman, L., and A. L. Adams. 1986. Adsorption of proteins out of plasma and solutions in narrow spaces. *J. Colloid. Interface Sci.* 111:391-402.
4. Macritchie, F. 1978. Proteins at interfaces. *Adv. Protein Chem.* 32:283-325.
5. Norde, W. 1986. Adsorption of proteins from solution at the solid-liquid interface. *Advan. Colloid Interface Sci.* 25:267-340.
6. Horbett, T. A., and J. L. Brash. 1987. Proteins at interfaces: current issues and future prospects. *ACS (Am. Chem. Soc.) Symp. Ser.* 343:1-33.
7. Schulz, G. E., and R. H. Schirmer. 1979. Principles of Protein Structure. Springer Pub. Co., New York. 149-161.
8. Torchinsky, Y. M. 1981. Sulfur in Proteins. Pergamon Press Inc., New York.
9. Matsumura, M., W. J. Becktel, and B. W. Matthews. 1988. Hydrophobic stabilization in T4 lysozyme determined directly by multiple substitutions of Ile 3. *Nature (Lond.)*. 334:406-410.
10. Perry, L. J., and R. Wetzel. 1984. Disulfide bond engineered into

- T4 lysozyme: stabilization of the protein toward thermal inactivation. *Science (Wash. DC.)*. 226:555-557.
11. Malcolm, B. A., S. Rosenberg, M. J. Corey, J. S. Allen, A. De Baetselier, and J. F. Kirsch. 1989. Site-directed mutagenesis of the catalytic residues Asp-52 and Glu-35 of chicken egg white lysozyme. *Proc. Natl. Acad. Sci. USA*. 86:133-137.
  12. Osserman, E. F., R. E. Canfield, and S. Beychok, editors. 1974. *Lysozyme*. Academic Press, Inc., New York.
  13. Dayhoff, M. O. 1972. Lactalbumine and lysozyme. In *Atlas of Protein Sequence and Structure*. Vol. 5. National Biomedical Research Foundation, Washington D.C. D139-D140.
  14. Stryer, L. 1981. Mechanisms of enzyme action: lysozyme and carboxypeptidase. In *Biochemistry*. 2nd ed. Freeman Publications, San Francisco. 135-155.
  15. Blake, C. C. F., D. F. Koenig, G. A. Mair, A. C. T. North, D. C. Phillips, and V. R. Sarma. 1965. Structure of hen egg-white lysozyme. *Nature (Lond.)*. 206:757-761.
  16. Bechtel, W. J., and W. A. Baase. 1987. Thermal denaturation of bacteriophage T4 lysozyme at neutral pH. *Biopolymers*. 26:619-623.
  17. Robson, B., and J. Garnier. 1986. *Introduction to Proteins and Protein Engineering*. Elsevier Science Pub. Co., Inc., New York. 155-194.
  18. Bergmeyer, H. U. 1984. *Methods of Enzymatic Analysis*. Vol. IV. Verlag Chemie Gmb H, Weinheim. 189.
  19. Hirschfeld, T. 1965. Total reflection fluorescence (TRF). *Can. Spectrosc.* 10:128.
  20. Harrick, N. J., and G. I. Loeb. 1973. Multiple internal reflection fluorescence spectrometry. *Anal. Chem.* 45:687-691.
  21. Thompson, N. L., T. P. Burghardt, and D. Axelrod. 1981. Measuring surface dynamics of biomolecules by total internal reflection fluorescence with photobleaching recovery or correlation spectroscopy. *Biophys. J.* 33:435-453.
  22. Axelrod, D., T. P. Burghardt, and N. L. Thompson. 1984. Total internal reflection fluorescence. *Annu. Rev. Biophys. Bioeng.* 13:247-268.
  23. Ausserre, D., H. Hervet, and F. Rondelez. 1985. Concentration profile of polymer solutions near a solid wall. *Phys. Rev. Lett.* 54:1948-1951.
  24. Cuypers, P. A., W. T. Hermens, and H. C. Hemker. 1978. Ellipsometry as a tool to study protein films at liquid-solid interfaces. *Anal. Biochem.* 84:56-67.
  25. Ivarsson, B. A., P. O. Hegg, K. I. Lundström, and U. Jönsson. 1985. Adsorption of proteins on metal surfaces studied by ellipsometric and capacitance measurements. *Colloids and Surf.* 13:169-192.
  26. Zimmermann, R. M., C. F. Schmidt, and H. E. Gaub. 1989. Absolute quantities and equilibrium kinetics of macromolecular adsorption measured by fluorescence photobleaching in total internal reflection. *J. Colloid Interface Sci.* In press.
  27. Axelrod, D., D. E. Koppel, J. Schlessinger, E. Elson, and W. W. Webb. 1976. Mobility measurement by analysis of fluorescence photobleaching recovery kinetics. *Biophys. J.* 16:1055.
  28. Peters, R., A. Brünger, and K. Schulten. 1981. Continuous fluorescence microphotolysis: a sensitive method for study of diffusion processes in single cells. *Proc. Natl. Acad. Sci. USA*. 78:962-966.
  29. Thompson, N. L., H. M. McConnell, and T. P. Burghardt. 1984. Order in supported phospholipid monolayers detected by the dichroism of fluorescence excited with polarized evanescent illumination. *Biophys. J.* 46:739-747.
  30. Miehlich, R. 1989. Adsorptionskinetik von Makromolekülen an Festkörperoberflächen und Grenzflächenphänomene strömender Polymerlösungen. Ph.D. thesis. Technical University, Munich. 28-35.
  31. Rabe, J. P., and W. Knoll. 1986. An ellipsometric method for the characterization of macroscopically heterogeneous films. *Optics Comm.* 57:189-192.
  32. Price, N. C., and G. K. Radda. 1972. A fluorogenic reagent as a probe for the subunit structure of glyceraldehyde-3-phosphate dehydrogenase. In *Structure and Function of Oxidation-Reduction Enzymes*. A. Akeson and A. Ehrenberg, editors. Pergamon Press, Inc., New York. 161-169.
  33. Hiramatsu, M., N. Okabe, and K. Tomita. 1973. Preparation and properties of lysozyme modified by fluorescein-isothiocyanate. *J. Biochem (Tokyo)*. 73:971-978.
  34. Charlwood, P. A. 1957. Partial specific volumes of proteins in relation to composition and environment. *J. Am. Chem. Soc.* 79:776-781.
  35. Horsley, D., J. Herron, V. Hlady, and J. D. Andrade. 1987. Human and hen lysozyme adsorption: a comparative study using total internal reflection fluorescence spectroscopy and molecular graphics. *ACS (Am. Chem. Soc.) Symp. Ser.* 343:290-305.
  36. Privalov, P. L., and N. N. Khechinashvili. 1974. A thermodynamic approach to the problem of stabilization of globular protein structure: a calorimetric study. *J. Mol. Biol.* 86:665-684.